THE ONSET OF CORONAL MASS EJECTIONS

G. M. SIMNETT and R. A. HARRISON*

Department of Space Research, University of Birmingham, England

(Received 23 February, 1984; in revised form 25 April, 1985)

Abstract. This study addresses the onset of coronal mass ejections. From examination of sensitive X-ray images from the Solar Maximum Mission around the projected onset time of coronal mass ejections we identify two important new features: (1) there is usually a weak, soft X-ray enhancement 15–30 min prior to the linearly extrapolated chromospheric departure time of the ejection; (2) this activity is generally from two widely separated ($\geq 10^5$ km) parts of the Sun. Possible physical mechanisms for these phenomena are examined and it is concluded that a plausible explanation is that the initial energy release is converted first into kinetic energy of suprathermal protons, 10^2–10^3 keV. The protons are trapped in a large magnetic loop which later breaks open as the mass ejection; Coulomb losses are the destabilizing agent but the mass ejection is probably magnetically driven. Protons that escape into the loss cone will impact the loop footpoints to heat the upper chromospheric material to a sufficiently high temperature to generate the weak soft X-ray emission. There will also be an Hα signature, and this is observed in a number of events. There is in general no radio emission or hard X-ray emission accompanying the soft X-ray precursor. When the coronal mass ejection is followed by a flare, then this is generally from a point close to, but not identical to, one of the points with the earlier soft X-ray enhancement.

1. Introduction

With the advent of improved visible light observations of coronal transients and other coronal activity, several attempts have been made to establish the causal relationship between coronal mass ejections and other manifestations of solar activity around the times of solar flares (Jackson, 1981; Kerdraon *et al.*, 1983; Wagner, 1983; Gary *et al.*, 1984). Wagner (1983) in his review of the Annecy SERF Mass Motions Workshop in 1981 stresses that there is very good observational evidence to show that the ejections depart the chromosphere at least several minutes before the flare onset. There is a growing body of evidence to support the view that the transient and the flare are initiated separately.

One of the difficulties impeding a rapid advance of this subject has been that transients, or mass enhancements in the corona, are hard to detect against the normal solar luminosity and have not been monitored by spaceborne coronagraphs at altitudes below 1.5 $R_\odot$ (from the centre of the Sun). The vast majority, if not all, type II radio bursts are associated with coronal transients (Gergely, 1984), although the converse cannot be said. The type II radio burst is generally believed to be due to a shock wave propagating through the corona generated by the impulsive energy release which gives the normal signatures of a large Hα flare; it is of great interest to understand how the shock relates to the transient (if indeed it does). There are very few events where both the visible light and radio observations have been spatially resolved. In the event of 1980,

* Present address: High Altitude Observatory, NCAR**, Boulder, CO 80307, U.S.A.
** NCAR is sponsored by the National Science Foundation.

Solar Physics **99** (1985) 291–311. 0038–0938/85.15.

June 29, 02:33 UT, reported by Gary *et al.* (1984), it was discovered (a) that the coronal transient appeared to start several minutes *before* the onset of the type II related disturbance; (b) that there was a faint forerunner to the transient, moving outwards some 50% faster than it and without associated type II radio emission; and (c) that from an analysis of the electron densities required to explain both the coronagraph and radio observations, the shock was located in this event within the dense ejected matter. This latter point is somewhat contentious, as Wagner and MacQueen (1983) maintain that the type II speed was in fact greater than that of the transient, so that (c) was not true throughout the whole event.

In general, without spatial radio observations the motion of the radio source must be derived from a model for the radio emission, e.g. plasma radiation at either the fundamental frequency or the second harmonic, plus a reasonable estimate for the coronal density. The latter is usually determined from the coronagraph observations which may be subject to some uncertainty in absolute sensitivity. Nevertheless, it has become increasingly clear (Wagner, 1983; Sawyer *et al.*, 1984; Gary *et al.*, 1984) that the coronal mass ejection starts some minutes before the type II shock is generated, although the latter frequently overtakes the leading edge of the transient. Gergely (1984) has addressed this point, and has concluded that most (but not all) type II burst velocities exceed that of the associated transient; also the average type II velocity is almost double the average transient velocity. This upholds the view that the two phenomena have quite different physical origins and should be considered unrelated in a physical sense, although the close temporal connection is not in doubt.

Supporting this interpretation is the work of Jackson (1981) who has shown that there is often, if not usually, a 'forerunner' region of enhanced density which is moving outwards ahead of the main transient. This led him to propose a model where the transient forerunner is initiated high ($3\ R_\odot$) in the corona, and the flare follows later. In this case, the conditions and radiation signatures of the initial phase of this process are of extreme importance to the understanding of the initial development of the flare. We have earlier studied the Hard X-Ray Imaging Spectrometer data (HXIS) from the Solar Maximum Mission (SMM) in 1980 during the early phase of events which did, or appeared to, generate a coronal transient (Harrison *et al.*, 1985). A link between pre-flare X-ray activity and coronal mass ejections was identified in this study. In this paper we have examined a large sample of the available data with a view to understanding the physical processes occurring at the Sun during this early phase. The results have shown the following:

(1) There is typically weak, soft X-ray activity in the form of a discrete event (not merely a gradual rise to a later event) some 15–30 min before the linearly extrapolated starting time of the transient in the low corona. We refer to this as the 'precursor'.

(2) This activity is frequently from widely separated points ($\geq 10^5$ km) on the Sun. When the transient is followed by a significant Hα flare, the flare is from close to one of these points.

In the following section we present data on nine events which were well observed by SMM, plus two more with similar X-ray signatures which occurred after the failure of

the SMM coronagraph. One feature of these events is that the hard (≥ 30 keV) X-ray emission from the precursor is minimal, i.e. below the sensitivity threshold of the Hard X-Ray Burst Spectrometer on SMM. The spectrum of the X-rays seen by HXIS is generally consistent with a low temperature thermal spectrum. ($T \leq (8 \pm 3) \times 10^6$ K) which supports the hypothesis that this emission is from a thermal plasma rather than from non-thermal electron bremsstrahlung. To elaborate on this last point, if the X-ray emission does not extend significantly above 5 keV then it follows that on the non-thermal hypothesis, the maximum energy of the hypothetical electron beam is of this order; such electrons have such a low range that they will be stopped in the corona and cannot propagate to widely separated points in the chromosphere.

We are therefore looking for a mechanism that will produce thermal X-ray emission at remote points on the Sun and destabilize a coronal transient. One such mechanism that has not been previously discussed, which we believe warrants serious consideration, is that the primary energy release is transferred predominantly into suprathermal protons of energies in the 10^2–10^3 keV range. Such energies are readily accomplished by minor shock acceleration. There may be some electrons above 5–10 keV, but certainly from an energetics viewpoint they may be neglected. Part of the accelerated proton population will be partially trapped in the coronal magnetic field and part will penetrate to the chromosphere. The former will heat the coronal gas and thereby destabilize the transient if the plasma $\beta \approx 1$, while the latter heat the chromospheric plasma responsible for the soft X-ray emission. This hypothesis is developed in Section 3.

2. Observations

We have chosen for our study nine coronal mass ejections/transients discussed by Wagner (1983), Lantos *et al.* (1981), House *et al.* (1981), Dryer (1982), Sawyer *et al.* (1984), and Stewart (1984), which occurred in the time period observed by HXIS in 1980*, plus two other events on September 24 and October 11 which had similar X-ray signatures but no confirmation of a coronal mass ejection (CME). The events are listed in Table I in two categories: the prime category, consisting of seven events, correspond to those which are directly applicable to the model outlined in Section 3; the other four events, which are more doubtful candidates, are included as they do have certain features which are consistent with the model. Presented in Table I are the times of the precursor and flare X-ray activity, the delay in minutes (where applicable), the radio signatures, SMM pointing and coincident Hα or X-ray activity on the visible solar disc. Two events discussed by the above authors are not included in our study for the following reasons: (1) The X-ray data for the May 5 CME were examined but there was no X-ray signature within the HXIS field of view prior to the detection of the event in the corona. (2) The April 27 CME had complex optical and X-ray data. There was a

* As all the events we discuss were in 1980, the year will be omitted from the text.

TABLE I

List of events

Date (1980)	Onset time (UT)		Delay (min)	Radio emission with		SMM pointing	Coincident activity on the disc
	precursor	flare		precursor	flare		
March 30	12:48	13:10	22		I	N24 E26	X-rays from remote point (1.4′)
May 6	08:59		22*	III RS		S18 W67	09:00–09:07 SN flare (S22 W06)
							09:01–09:12 SF flare (S18 W59)
June 27	21:50		14*	III		S28 W57	
June 29	02:12	02:33	21		II	S28 W72	X-rays from remote point (1.5′)
	10:25	10:41	16		II	S28 W76	
Sept. 24	07:07	07:32	25		II, IVm	N17 W34	X-rays from remote point (3.6′)
Oct. 11	17:05	17:40	35		III	S08 E30	X-rays from remote point (2.1′)
				Other events			
April 7	02:38	03:20	42	III	IV, IVm	N13 00	02:45–03:08 SF flare (S14 W70)
							02:45–03:15 SN flare (N23 E16)
							03:12–03:32 SF flare (N12 E40)
							03:14–06:47 2N flare (N30 W75)
April 12	?	20:38		III	II	N12 W77	19:47–20:23 SN flare (N21 W53)
							19:55–20:37 ?B flare (N11 W72)
							20:06–20:12 SF flare (S17 W68)
April 14	no data	04:33		Inter-mittent III		N13 W90	04:44–04:55 SF flare (N16 E32)
June 29	18:03	18:23	20	III	II	S28 W77	18:06–18:16 SF flare (S11 W36)

* Delay from extrapolated start of the CME (Sawyer *et al.*, 1985).

flare spray at the limb at 02:29 UT, while HXIS was observing the decay of an earlier event which included a fast spike ($\approx$ 90 s FWHM) at 02:23 UT.

As an example of the phenomenon we wish to discuss, Figure 1 shows the precursor soft X-ray activity at the solar limb on June 29, from 02:08–02:30 UT. An image of the HXIS coarse field of view (32″ resolution) taken from 02:12:48–02:26:45 UT is shown inset, with the approximate position of the limb indicated by the dotted line. The 3.5–5.5 keV X-ray intensities from regions *A* and *B* are plotted prior to the onset at

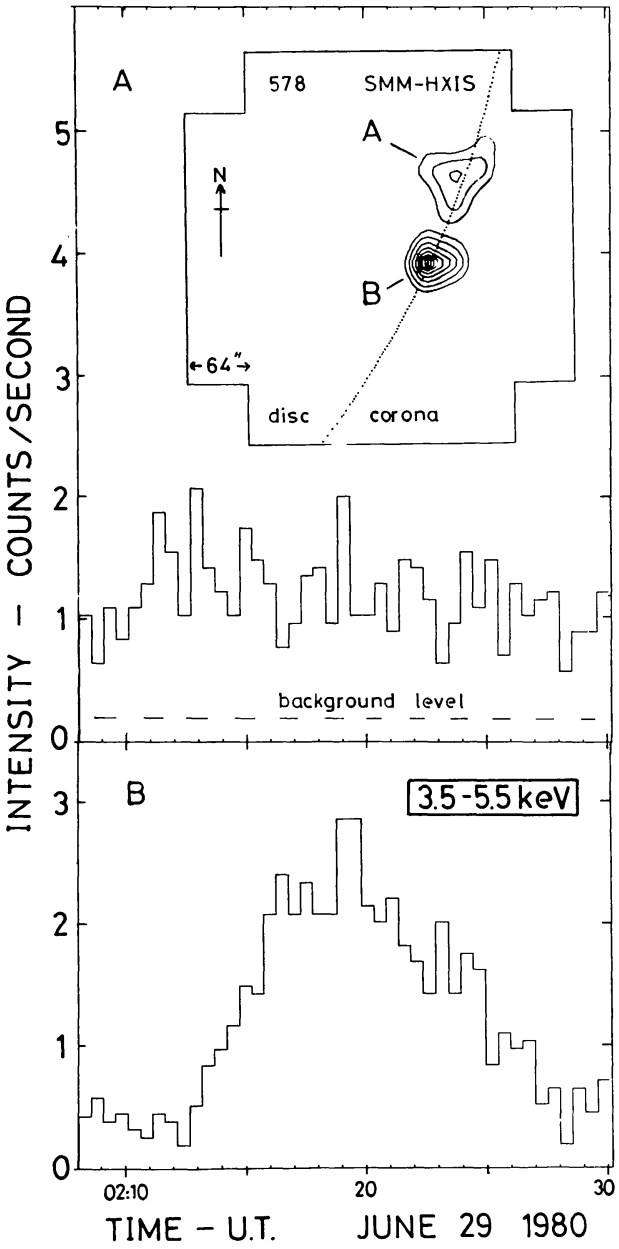

Fig. 1. The 3.5–5.5 keV X-ray activity from two widely separated points *A* and *B* on the SW limb on 1980, June 29, prior to the detection of a coronal mass ejection. Inset is the 3.5–5.5 keV image from 02:12:48–02:26:45 UT, which has a peak contour level at 578 counts/pixel. The contour levels are at 98, 90, 80, 70, 55, 40, 26, 14, 7, and 3%. A flare occurred in region *A*, with its impulsive phase at 02:32 UT.

02:32 UT of the GOES class M3 flare from region *A*. The intensity is enhanced first at *A*, before a more significant, but more transient, increase is detected from *B*. The regions *A* and *B* were identified as the footpoints of a large coronal loop by Harrison *et al.* (1984). The CME and associated type II radio burst have been discussed by Gary *et al.* (1984) who note (a) that a faint arc moves outwards ahead of the main CME, (b) that both it and the CME originate prior to the impulsive phase of the flare, and (c) that the type II shock propagated into the already-rising CME. There was no radio emission associated with the precursor X-ray activity, which precludes the presence of non-thermal electrons in the corona. This appears to be a general property of the precursor emission, although there are occasional exceptions.

The March 30 event has been reported by Lantos *et al.* (1981) who noted the connection between a white-light loop transient, a long duration X-ray event and a metric noise storm which started around 13:10 UT. The soft X-ray data again show coincident activity from different parts of the field of view some 22 min before the flare onset. Figure 2 shows the 3.5–5.5 keV X-ray intensity from two positions *A* and *B*, separated by around 1.4′ or around 70 000 km at the location of the region. There is a weak, broad increase from *A* and an impulsive increase from *B*, lasting around three minutes. There was no radio emission associated with this activity (A. O. Benz, private communication). The location of the subsequent flare was close to region *B*, although it was not bright enough or impulsive enough to classify as a flare in the *Solar-Geophysical Data* report (U.S. Department of Commerce). Apart from the metric radio noise storm, there was no other radio activity. Therefore this event may be caused by backward streaming particles accelerated in the shock associated with the outward moving CME, according to the model suggested by Simnett (1985).

Proceeding in chronological order down Table I, we now have two examples of weak, soft X-ray brightenings which were not followed by a significant flare but were nevertheless related to both a CME and an erupting filament. The event on May 6 (House *et al.*, 1981) was seen off the west limb close to the solar equator, and it extrapolated back to the low corona at 09:21 UT (Sawyer *et al.*, 1985). HXIS was pointing at S 18 W 67 and observed a small, impulsive and short lived (FWHM $\leq$ 1 m) soft X-ray brightening at 08:59 UT, which is plotted in Figure 3. There was no radio emission observed at this time. The spectrum of the burst is soft; from the ratio of counts in the 3.5–5.5/5.5–8.0 keV channels a temperature of $8.5 \pm 1.0 \times 10^6$ K is derived. This fact, the lack of radio emission and the rapid decay of the X-ray burst strongly suggests a chromospheric origin for the burst, with no electrons in the corona at that time. Shown inset in Figure 3 is the 0.5–4 Å full-Sun intensity-time history from the GOES satellite, which registered a small increase which peaked at around 09:05 UT. The relative sensitivity of the two scales may be judged by comparing the increases at 08:44 UT. It is clear that at 09:05 UT GOES was observing an event from outside the HXIS field of view. It is significant that two Hα subflares were reported at this time (see Table I). From 09:00:06 – $\approx$09:05 UT a group of reverse slope metric type III bursts was observed, with the strongest bursts occurring from 09:02:20–09:04:15 UT (A. O. Benz, private communication). Interpretation of these phenomena is given in Section 3.

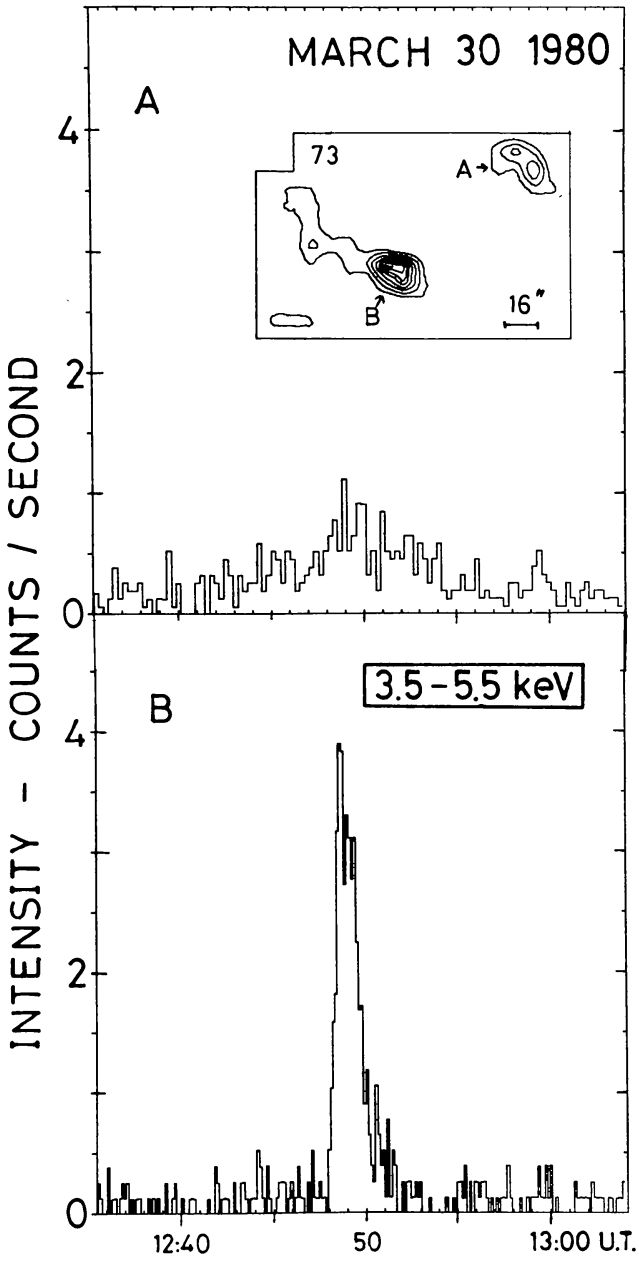

Fig. 2. The 3.5–5.5 keV X-ray activity from two widely separated points *A* and *B* on 1980, March 30, prior to the detection of a coronal mass ejection. Inset is the 3.5–5.5 keV image spanning the impulsive burst from *B*, and it has a peak contour level corresponding to 73 counts/pixel. The contour levels are 98, 90, 80, 70, 55, 40, 26, 14, and 7%.

On June 27 we observed weak soft X-ray activity with a time profile resembling a small, thermal flare (rise time ≈ 3 min, decay time ≈ 18 min), in coincidence with an erupting filament. This activity is probably similar to that found by Webb *et al.* (1976) from Skylab observations. Sawyer *et al.* (1985) report a CME from the south–west limb which extrapolated back to the low corona at 22:04 UT. There was no accompanying flare, but owing to the proximity of the limb and the remote connections for some of the events in Table I, this could be behind the limb. Weak metric type III bursts were observed for several hours around this time. For both this event and that of May 6, the

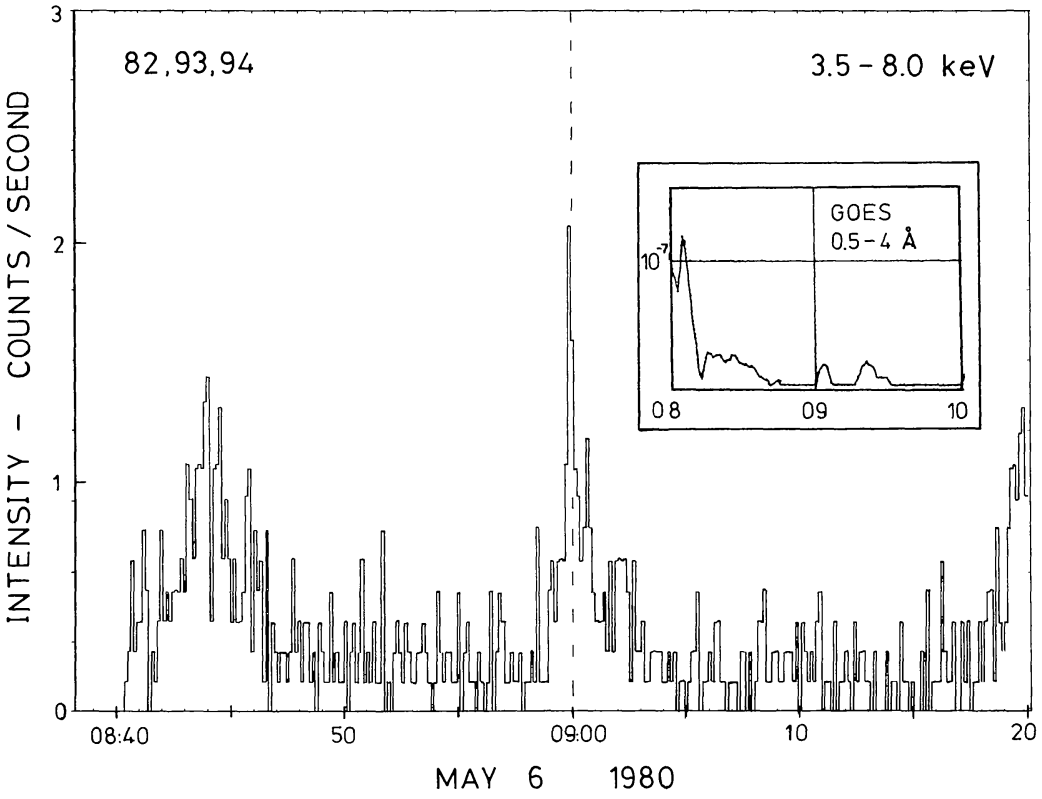

Fig. 3. The intensity of 3.5–8.0 keV X-rays, from ≈08:40–09:20 UT on 1980, May 6, of three 32″ × 32″ pixels from the HXIS coarse field of view. The pixel numbers in the detector array are 82, 93, and 94. The spike at 08:59 UT is spatially unresolved but is consistent with a lateral extent of ≤16″. Inset is the 0.5–4 Å X-ray intensity of the full Sun from the GOES satellite from 08:00–10:00 UT.

delay between the precursor and the subsequent activity, in these cases the CME's, is calculated from the extrapolated start time of the CME.

For the listed event at 10:25 UT on June 29, discussed by Harrison *et al.* (1985), there were no observations made by the Coronagraph/Polarimeter on SMM. However, the flare at 10:41 UT produced a strong type II radio burst so that it is reasonably certain that a CME did take place (Gergely, 1984). This view is supported by interpretation of post-flare images of the corona (A. J. Hundhousen, private communication). The precursor activity was not at the same point as the main flare, but around 32″ away. As the flare was virtually on the limb, further interpretation regarding spatial effects is difficult.

The events of September 24 and October 11 were not observed by the Coronagraph/Polarimeter on SMM, but were interpreted as CME events from ground-based data. Figure 4 shows the intensity-time history of 3.5–8.0 keV X-ray emission from two widely separated regions *A* and *B* for the September 24 event. *B* was near the easterly end of a large active region, Hale 17145, of area 4400×10^{-6} of a solar hemisphere and inset in Figure 4 is the 3.5–5.5 keV X-ray image from 07:06:54–07:13:14 UT showing the spatial structure of the region. The centroid of the 1B flare is marked with an 'X' in Figure 4 (inset), and it was displaced approximately 40″ SE of the brightest point in the precursor activity. It was accompanied by a type II radio burst. There were also

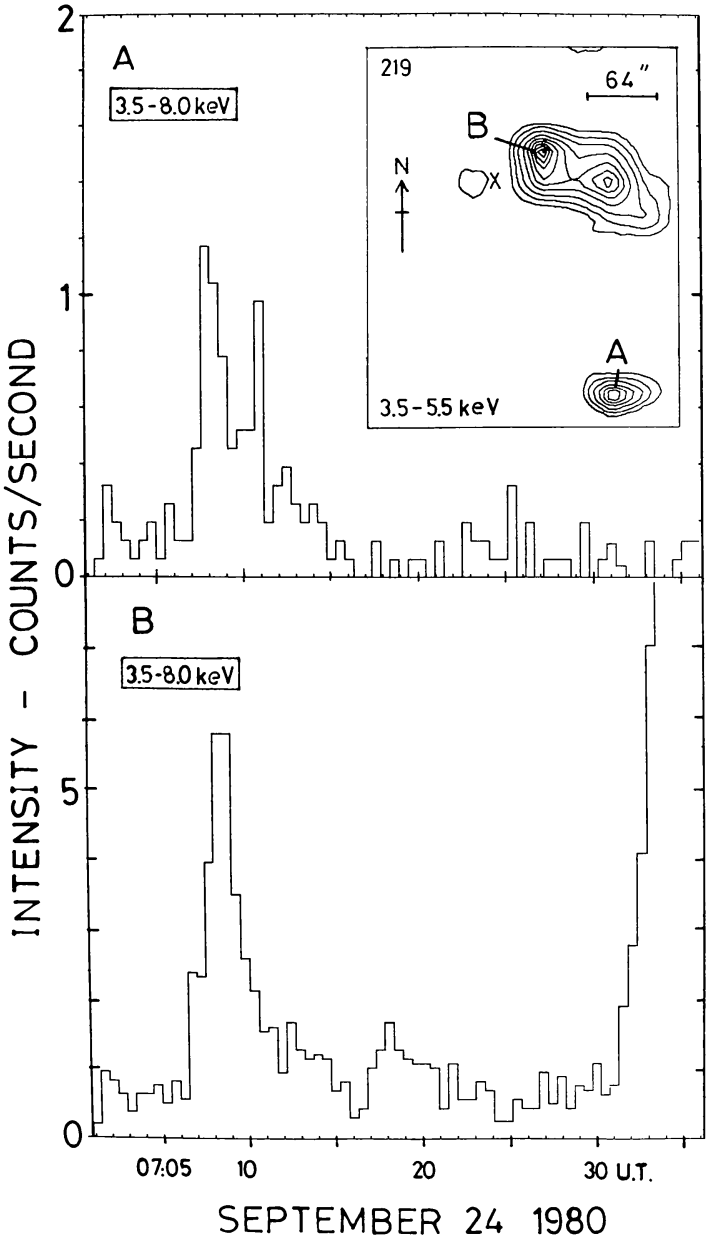

Fig. 4. The 3.5–8.0 keV X-ray activity from two widely separated points *A* and *B* from 07:01–07:36 UT on 1980, September 24. Inset is the 3.5–5.5 keV image from 07:06:54–07:13:14 UT, which has a peak contour of 219 counts/pixel. The contout levels are 98, 90, 80, 70, 55, 40, 26, 14, 7, and 3%. The location of the subsequent flare is marked with an '×'.

type III bursts both accompanying the impulsive phase and preceding it at 07:28:20 UT; however, there was a weak pre-flare X-ray increase with a hard spectrum seen from around 07:27 UT. There was no radio emission observed during the precursor activity. The close temporal association of soft X-ray emission at around 07:08 UT from both *A* and *B*, separated by some 160 000 km, suggests that they are linked in some way, and the most plausible association is via a high coronal arch.

The event on October 11 occurred in Hale region 17188, then at S 08 E 30. This was the largest active region, area 8000×10^{-6} of a solar hemisphere, visible in October 1980. Figure 5 shows the 3.5–5.5 keV intensity-time profiles for three resolved sources

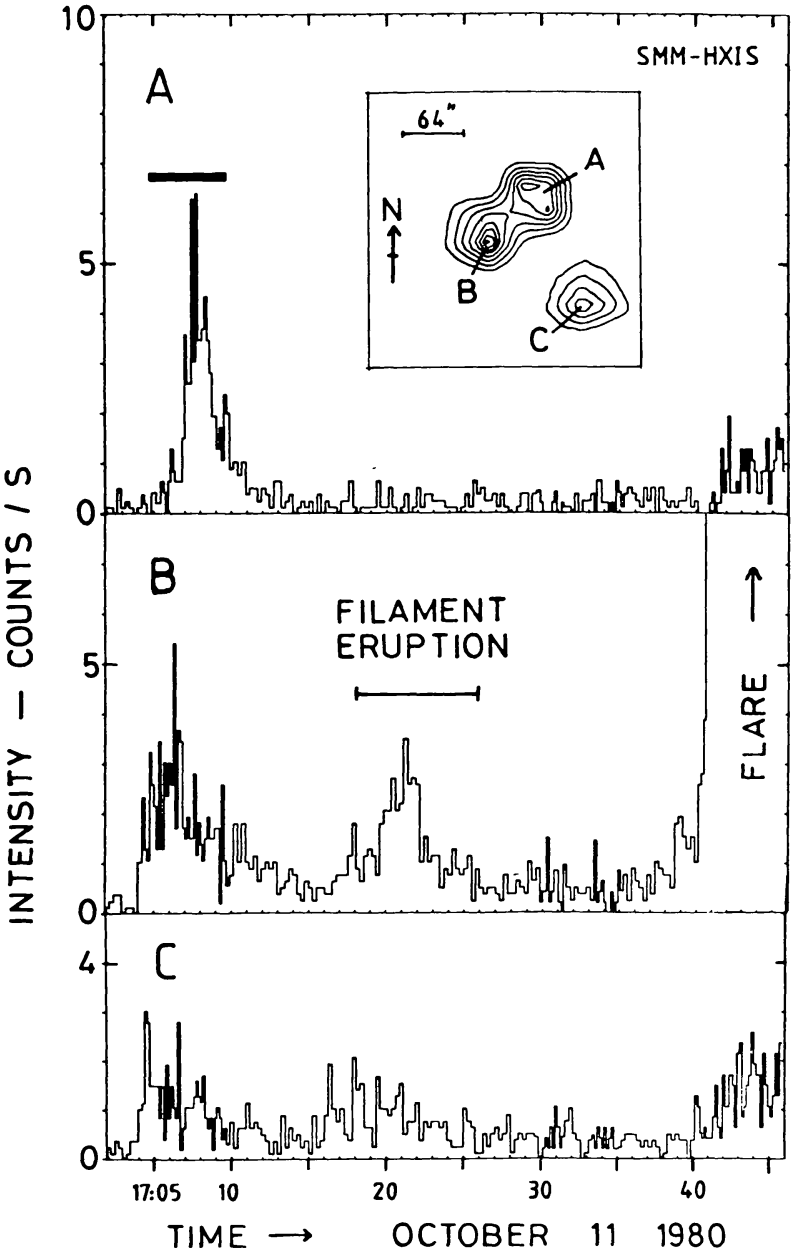

Fig. 5. The 3.5–5.5 keV X-ray activity from three widely separated points *A*, *B*, and *C* from 17:02–17:46 UT on 1980, October 11. Inset is the 3.5–5.5 keV image spanning the main burst from location *A* from 17:04:55–17:09:35 UT. A filament eruption coincided with a secondary soft X-ray brightening from point *B*, which was followed at 17:40 UT by a flare.

A, *B*, and *C*, with their relative positions shown inset for the period 17:04:55–17:09:35 UT. At around 17:03 UT there was weak emission from regions *B* and *C*, and before this had decayed there was a weak burst from *A*. At 17:17 UT there was a filament eruption that was accompanied by weak activity in both *B* and *C*. The class −B flare erupted from B, starting with a gradual rise from around 17:36 UT and an impulsive phase at 17:41 UT, which included a microwave burst of 149×10^4 Jy at 9.4 GHz. This event is included in Table I because we assume the filament eruption is

indicative of a CME. This event has some obvious similarities to the September 24 event, and is probably a manifestation of the same physical process. There was no radio activity associated with the precursor emission at 17:03–17:10 UT; however there was a weak group of type III bursts at 17:25 UT, followed by further groups of type III's at 17:35–17:36 UT and 17:39–17:40 UT.

The characteristics of the primary set of events may be summarized as follows:

(1) In five out of seven events there is weak soft X-ray activity from widely separated points (see Table I) in the preceding half hour.

(2) In the five events that were followed by a flare, there was no radio emission associated with the precursor activity; in one of the others, May 6, there was no radio emission at the time of the first narrow X-ray burst, but reverse slope type III bursts were detected in coincidence with the X-ray emission from the remote point.

(3) The delay between the precursor X-ray activity and either the onset of the main flare (when this occurs) or the extrapolated onset of the CME is in the range 14–35 m.

(4) The flare is, in general, not from precisely the same location as one of the precursor brightenings, but from close to one of them ($\leq 40''$).

(5) There are no hard X-rays ≥ 15 keV associated with the precursors at the sensitivity level of HXIS (Van Beek *et al.*, 1980).

2.1. The secondary events

There were four other events where X-ray activity was observed prior to the onset of the CME, but in each case it is uncertain whether the associations are merely coincidental.

The April 7 event has been discussed by Wagner (1983) who argued that the most probable departure time of the CME preceded the associated flare by about 10 min. In this event there was a significant amount of coincident Hα activity from several widely separated parts of the Sun. The flare associated by Wagner with the CME was a class 2N flare from Hale region 16740, then at N 30 W 75, which started at 03:14 UT. HXIS was observing region 16747, then close to disc center and the 3.5–5.5 keV X-ray intensity is shown in Figure 6 from 02:35–03:25 UT. Inset is the X-ray image during the onset of the small brightening seen near the start of the time period. It is interesting to note that there were two simultaneous subflares (see Table I) from parts of the Sun separated by around 90° at the time of this weak X-ray brightening from disc centre. Again, for the main flare, there was a simultaneous subflare from 03:12–03:32 from N 12 E 40, and the X-ray activity (plotted in Figure 6) from disc centre. To complete the connection, the maximum phase of the flare associated by Wagner with the CME was at 05:34 UT, essentially coincident with the maximum phase of a class 1B flare from region 16747, which had its impulsive phase at 05:29 UT.

We suggest from these coincident activities that the observed CME originated in a very large coronal structure linking region 16740 to the complex of regions 16747/16752, with some possible lesser connections to the regions responsible for the subflares given in Table I. Regions 16747/16752 were later observed by HXIS to be linked by a large

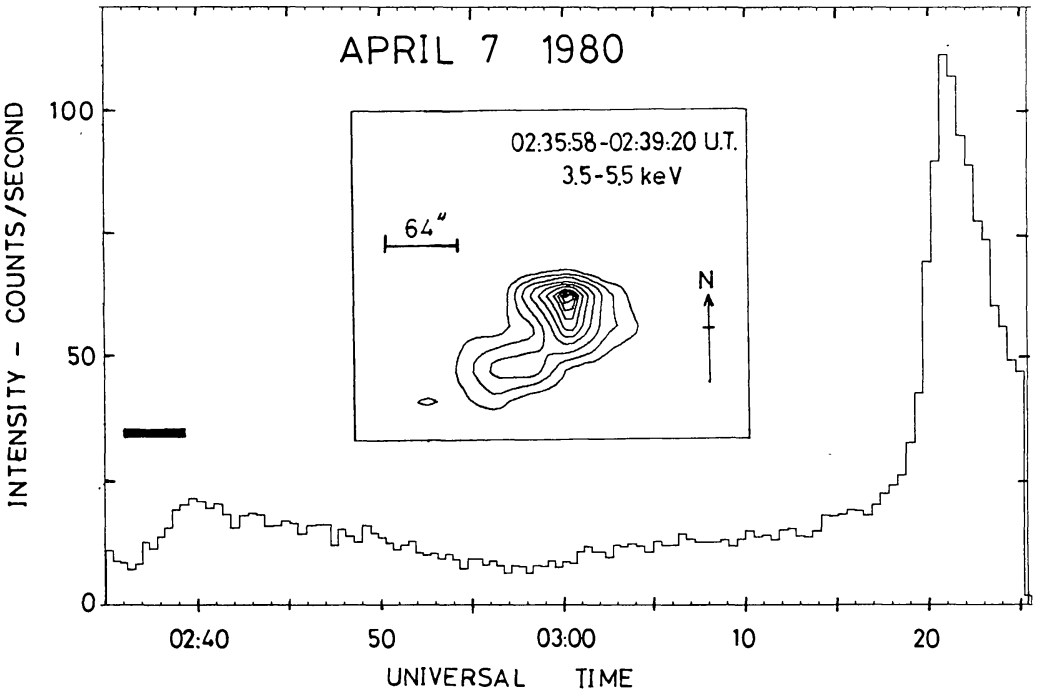

Fig. 6. The 3.5–5.5 keV X-ray activity from Hale region 16747 at the centre of the visible solar disc in coincidence with activity elsewhere on the Sun (see text). The X-ray emitting structure from 02:35:58–02:39:20 UT is shown inset, and it spans around 2′.

X-ray emitting arch. However, the important point with regard to the present study is that there is activity prior to the CME from widely separated locations.

The event on April 12 has been discussed by Sawyer *et al.* (1984) and is included on our list primarily because it occurred when Hale regions 16747 and 16752 were (a) close to the west limb, (b) connected by a soft X-ray emitting arch, and (c) were active with small flares prior to the CME. The X-ray activity from these flares reached the GOES C5 level, they included type III bursts and were observed to energize a large, low coronal loop (Rust *et al.*, 1985). Thus there was a hierarchy of magnetic loops clearly visible in soft X-rays at this time, with the bulk of the hot plasma from the early, small flares confined to the lower loops. It is sufficient to note here that the CME occurred from the general location of a large coronal structure linking two regions separated by over 200 000 km, which was overlying a smaller structure within one of the regions in which there had been non-impulsive soft X-ray activity in the 45 m preceding the extrapolated onset of the transient.

The April 14 event occurred when SMM was pointing at the west limb; Figure 7 shows an image of the north-west limb taken with 3.5–5.5 keV X-rays from 04:02:23–04:15:03 UT. The position of the limb is indicated and it is clear that there was weak activity from points *A* and *B* around the limb, extending into the corona. The extrapolated starting time of the CME was 04:00 UT (Sawyer *et al.*, 1985) and it occurred almost totally over the solar north pole. If we use the result of the delay time between precursor and CME onset derived above, the SMM was in the Earth's shadow during the appropriate period. However, as the transient left the Sun, there were weak,

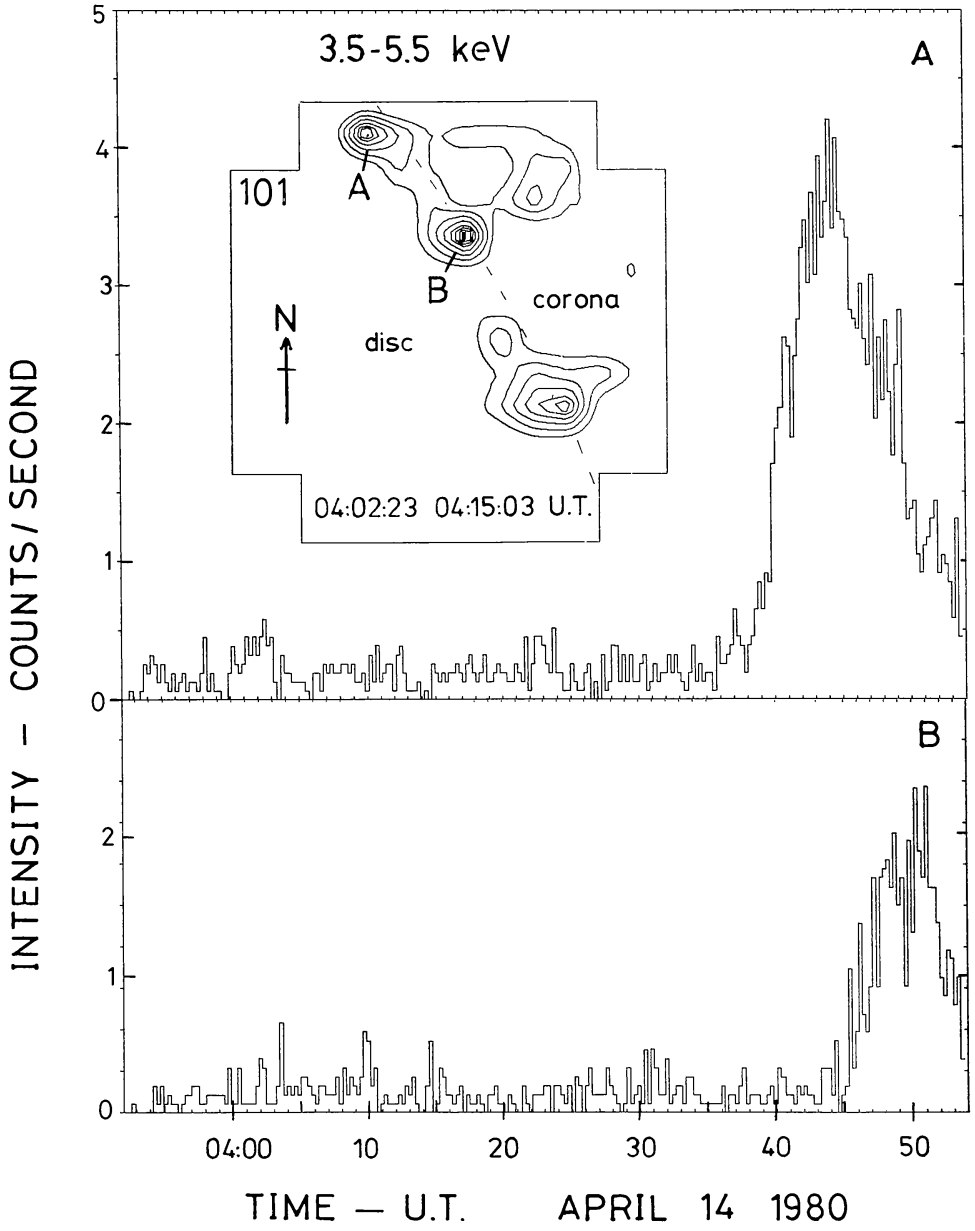

Fig. 7. The 3.5–5.5 keV X-ray activity from the NW solar limb from 03:52–04:54 UT on 1980, April 14. Inset is the image obtained from 04:02:23–04:15:03 UT, showing a bright coronal arch, *C*, linking two bright points *A* and *B*. The X-ray emission from the southerly region *D* remained approximately constant throughout. The activity from *B* is precisely coincident with a subflare from N 16 E 32.

non-impulsive increases from regions *A* and *B* together with a subflare from N 16 E 32, at 04:44–04:55 UT, which is *precisely* coincident with the brightening from *B*. The edges of the CME are consistent with the legs of a loop at N 16 E 32 and on the NW limb, although because of projection effects other possibilities are not excluded.

The final event occurred on June 29 at 18:03 UT and has been discussed by Harrison *et al.* (1985). It occurred when the active regions involved with the major flares were right on the west limb, and therefore it is difficult to resolve the structures spatially. However, the only discrepancy between this event and those in the upper part of Table I was the

magnitude of the precursor, as it was a small, impulsive flare, with decimetric type III bursts and hard X-rays. In all other respects it fits perfectly within the properties summarized above, which leads us to suggest that in some instances, the precursor activity may be energetic enough to produce a flare.

As mentioned in the Introduction we expect some electron acceleration might accompany the proton acceleration. Ground-based radio telescopes are sensitive enough to detect very low fluxes of electrons in the corona; therefore the detection of type III radio emission does not in any way indicate that an energetically-dominant electron population exists. However, events where there is an absence of type III emission would seem to be preclude the presence of non-thermal electrons at an intensity, or with a velocity spectrum, conducive to excitation of plasma radiation. Apart from this, it is difficult to known how the type III radiation, when observed, fits into our model. The latter is developed from an energetics viewpoint, and in such a framework the energy in the type III burst electrons is not significant.

3. Interpretation

In this section we develop a model which is aimed at explaining all the phenomena we have identified with the seven prime examples given in Table I. As a premise we suppose that the various emissions seen at the Sun over a timescale of the same magnitude as a typical event duration are causally related. For example, for the March 30 precursor event shown in Figure 2, the emissions that both reach a maximum around 12:49 UT would be considered causally related.

3.1. Evaluation of the relevant parameters

We need first to establish what is responsible for the precursor X-ray emission, as it generally has no radio signature, which precludes energetic electrons in the corona, and yet widely separated parts of the Sun exhibit temporally coincident activity, which would have a natural explanation if they were connected by a coronal magnetic loop. We adopt as a working hypothesis the concept (Heyvaerts *et al.*, 1977). that energy release occurs when two magnetic loops merge somewhere in the corona, and that energy is transferred into non-thermal particles. The transfer mechanism could be via small shocks generated by turbulence in the current sheet associated with the merging magnetic flux, and it is likely that particle acceleration occurs in the shocks by the mechanism suggested by Bell (1978).

This situation is illustrated schematically in Figure 8a, where the accelerated particles move both upwards and downwards from the acceleration region according to the side of the shock from which they escape. The shock acceleration mechanism is primarily velocity dependent, which results in the bulk of the energy being transferred to protons (this term is used to include all ion species) rather than electrons. Traditionally this has not been interpreted as they way particle acceleration proceeds in flares, so it is worth discussing this point in more detail.

Electrons have generally been considered the dominant non-thermal species during

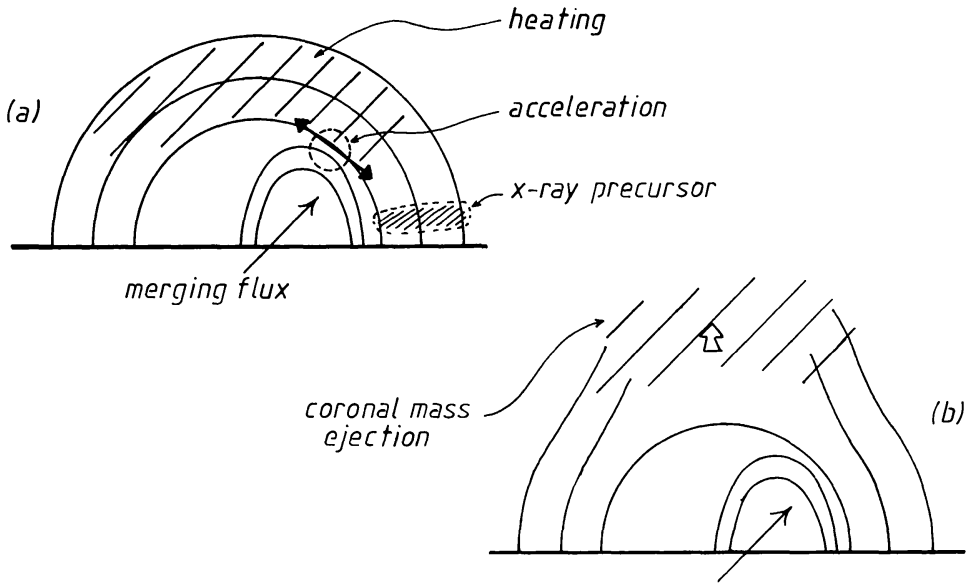

Fig. 8. A schematic representation of the geometry of the coronal mass ejection onset. (a) Acceleration occurs in a region of merging magnetic flux, resulting in coronal heating and the initiation of the soft X-ray precursor. (b) Following heat input from the protons, the thermal pressure exceeds the magnetic pressure in the loop and the plasma is no longer confined.

the onset of flares primarily from observations of type III radio emission and impulsive hard X-ray bursts, and theoretical arguments based on energetics (Lin and Hudson, 1976). There is no doubt that type III bursts are produced by beams of non-thermal electrons, but the energy requirement for these are small compared with the flare energy budget. The situation is more controversial for the hard X-rays, as the energy requirement is comparable with the total flare energy if non-thermal bremsstrahlung is the cause. However, in the precursor events there are no hard X-rays and in most of them (5 out of 7) no radio signature. Therefore there is no *observable* that appears to require the presence of an energy-dominant non-thermal electron population in the precursor phase.

If we take this argument one stage further, we can ask if the plasma producing the soft X-ray bursts could be heated by non-thermal electrons? The spectra are consistent with emission from a thermal plasma at $(8 \pm 3) \times 10^6$ K and the rapid decay times seen in some events, such as May 6 and March 30, require chromospheric densities if the emission is thermal. It must be remembered that the X-ray emission itself cannot be non-thermal bremsstrahlung unless it is thin target emission, as the bulk of the energy in thick target emission is dissipated as heat, which would raise the plasma temperature to the region of that observed. Thin target emission is eliminated as the escaping electrons would generate radio emission in the corona. If the emission is thermal, and the heating is by electrons impacting the chromosphere, we can ask what energy electron is required to reach that depth? For any reasonable atmosphere model above an active region the threshold energy for electrons to reach the chromosphere is around 30 keV. Therefore, if energy deposition is in the chromosphere from a beam of electrons these should have energies ≥ 30 keV, and some hard X-rays ≥ 30 keV should be produced.

As the hard X-rays at the time of the precursors are entirely absent (Dennis *et al.*, 1983; B. R. Dennis, private communication) this appears to eliminate electrons as the primary energy source for heating the plasma.

We therefore return to the predicted major energy carrier following shock acceleration, namely the protons. The downward moving protons are treated first. They will lose energy and scatter through Coulomb collisions with the ambient medium, and some will charge-exchange to produce fast, excited neutral hydrogen. The critical parameter is the column density above the transition zone and this will clearly be a function of the model atmosphere chosen. As we are considering only active regions which have been flaring recently, the atmospheres derived by Basri *et al.* (1979) and by Machado *et al.* (1980) (flare model F1) will be used as limiting cases. These correspond to mass column densities of 1×10^{-4} and 3×10^{-4} g cm^{-2}, respectively (Machado *et al.*, 1980), and the threshold proton energies, E_T, required to penetrate such a thickness of hydrogen are 300 keV and 570 keV.

In the past there has been considerable discussion of the role of protons in flare development (Elliot, 1964). Švestka (1970) and Najita and Orrall (1970) concentrated on the production of white light in strong flares by protons of energies ≥ 10 MeV. Orrall and Zirker (1976) raised the possibility that low energy protons, $E \leq 1$ MeV, might be important and they suggested an observational test that relied on charge exchange reactions in hydrogen, followed by red-shifted Ly α radiation. An attempt to detect this (Canfield and Cook, 1978) has not been successful; however the cross sections are energy dependent and only become important at low energies, $\ll 100$ keV. Therefore if the bulk of the energy in the accelerated protons is ≥ 100 keV, the sensitivity of this technique is reduced.

Once a 300 keV proton has penetrated below the transition zone, it is stopped within 100–200 km (if we adopt the F1 atmosphere of Machado *et al.* (1980)) in a fraction of a second. Such a proton will only be slightly more energetic at the acceleration site in the corona. Even protons of a few MeV will deposit their energy in the top few hundred km of the chromosphere. If the beam strength is high enough, plasma will be heated sufficiently to produce a soft X-ray event.

How much energy is required to heat the top of the chromosphere to a sufficient temperature to produce the precursor X-ray burst? In the hottest precursor observed, at 02:12 UT on June 29, HXIS measured a temperature T of $11 \pm 1 \times 10^6$ K, with an emission measure Y of $(3.1 \pm 0.4) \times 10^{46}$ cm^{-3}. If the density of the plasma is in the region 10^{11}–10^{12} cm^{-3}, then the energy content Q of the plasma, given by $Q = 3YkTn_e^{-1}$, is in the region 10^{26}–10^{27} erg; k is Boltzmann's constant, and the lower value corresponds to the higher density. This energy input is typical for the precursors discussed above.

In the situation shown in Figure 8a, it is expected that around half the particles move upwards and that those with small pitch angles will travel around the loop to the remote footpoint, providing that they are sufficiently energetic to penetrate the mass within the loop. These particles provide the energy for the chromospheric response at the remote footpoint and the relative strength and timing of the two responses will depend on the

physical parameters describing the acceleration and the coronal loop. Particles with large pitch angles, moving in either direction, will mirror before reaching the chromosphere, and therefore will be likely to deposit *all* their kinetic energy in the corona, via Coulomb collisions, thereby heating the coronal gas within the loop. Protons are particularly suited to this, as they have a favourable energy loss per unit mass traversed at the energy we are concerned with, 10^2–10^3 keV.

This must now be related to the coronal mass ejection. Pneuman (1980) has suggested that CME's are magnetically driven through a typical coronal helmet structure; an increase in field strength below the helmet could easily propel the overlying magnetic field to infinity, taking the mass with it. Clearly just before this happens a metastable equilibrium must exist, where the magnetic driving force is balanced by gravity and magnetic tension. As gravity does not change, then either an increase in the driving force or a reduction in magnetic tension in the helmet structure may destabilize the structure. We suggest that heating of the coronal gas by Coulomb losses of the accelerated protons exerts an increased pressure on the overlying field, reducing the tension and causing loss of equilibrium. An advantage of this process is that no increase in field strength is required; this appears to be significant as any energy release which resulted in precursor activity should, naively, result in a decrease in field strength. A typical time scale of this process is the stopping time of a 500 keV proton, which in a mean density of 4×10^8 cm^{-3} is around 9 m, or in a density of 2×10^9 cm^{-2}, around 2 m. These times are sufficiently short that the heat liberated will not be radiated or conducted away, instead of raising the temperature of the coronal gas.

An important property that protons have over electrons is that for energies in the region, say, 30 keV–1 MeV, Coulomb losses/thickness of matter traversed are some orders of magnitude higher. For example, a proton of 200 keV may be completely stopped by passing through 4.6×10^{-5} g cm^{-2} of hydrogen, whereas a 200 keV electron would lose only 0.27 keV in the same thickness. Therefore protons have the potential for depositing energy in a low coronal loop which is unparalleled. Although in principle electrons could bounce backwards and forewards many times in a magnetic loop, in practice pitch angle scattering removes them to the footpoints before they have lost a significant fraction of their energy.

We now show that for reasonable values of the density and altitude of the coronal loop, the losses of the accelerated protons are primarily in the corona. Suppose the looptop is at a height h cm above the photosphere, and that the mean density is $\bar{\rho}$ cm^{-3}. The loop is assumed to be semicircular and filled with hydrogen. The matter M g cm^{-2} traversed by a charged particle going around the loop is then

$$M = \pi h \bar{\rho} m_p P \quad \text{g cm}^{-2},$$

where P is a factor ≈ 2 introduced to account for proton pitch angle and m_p is the atomic mass unit. Some typical values are given in Table II, where the coronal densities are in the range given by Stewart (1976) based on studies of metric radio bursts. It is apparant from Table II that for protons of energies up to ≈ 1 MeV, trapping on a coronal loop will quickly result in the loss of all their kinetic energy through Coulomb collisions. The

TABLE II

Energy/range values for protons in a coronal loop

Mean density $\bar{\rho}$ (cm^{-3})	Looptop height (cm)	Mass traversed (M g cm^{-2})	Proton energy for range M
4×10^8	5×10^9	2.1×10^{-5}	130 keV
	10^{10}	4.2×10^{-5}	190 keV
2×10^9	5×10^9	1×10^{-4}	310 keV
	10^{10}	2×10^{-4}	460 keV

energy content in the spectrum above 1 MeV is likely to be a small percentage of the total energy in the spectrum. The scenario outlined in Figure 8a evolves to that shown in Figure 8b, and the proton heating triggers the CME.

One final parameter needs to be evaluated, namely the amount of energy deposition required to reduce the magnetic tension in the coronal helmet. This will occur when the thermal pressure becomes greater than the magnetic pressure, i.e. when $\beta \geq 1$, but unfortunately we do not know the starting conditions. It is informative to calculate how much energy is required to produce a 10^6 K temperature increase. It will then be a matter of speculation to gauge whether this amount of heating is sufficient to destabilize the structure. However, if the initial condition is $\beta \lesssim 1$, then a 10^6 K change should be the right *order of magnitude*.

The energy, Q ergs, required to heat the coronal gas through an increment in temperature ΔT is

$$Q = \bar{\rho} V k \Delta T \quad \text{ergs},$$

where V is the volume of the structure. If we take $V = 10^{29}$ cm^3, $\bar{\rho} = 4 \times 10^{-8}$ cm^{-3} and $\Delta T = 10^6$ K, then $Q \approx 5 \times 10^{27}$ erg. This is not an unreasonable energy, and it is greater than, but comparable to the estimate of the energy in the soft X-ray precursor. There is, of course, no reason a priori to suppose that these estimates should be comparable.

To summarize, we have shown that energy losses of protons in the 10^2–10^3 keV range are very efficient at heating the gas in a coronal loop. Further, an energy input of a few $\times 10^{27}$ erg is sufficient to raise the temperature of a 10^{29} cm^3 volume of the corona by $\approx 10^6$ K, which we believe must be the right order of magnitude to lead to a significant change in β.

3.2. Overview of the Total Situation

We have demonstrated above that protons in the energy region 10^2–10^3 keV have the right properties both to produce heating at widely separated points and to transfer significant amounts of energy to the coronal gas. With regard to the observations of CME's, they are often associated with a substantial flare, but as emphasized by Wagner (1983) and Wagner and MacQueen (1983), the CME trajectory frequently extrapolates back to the inner corona at a time prior to the start of the flare. Then the flare-associated

blast wave propagates outwards and may overtake the earlier generated CME. We believe the sequence of events is as follows:

(1) Energy release in the corona produces small shocks which accelerate protons and electrons, with the bulk of the energy residing in the protons.

(2) The protons heat the lower coronal gas beneath a magnetic helmet structure, or other closed configuration, and trigger a magnetically-driven mass ejection.

(3) The forerunner (see Jackson, 1981) is an MHD disturbance caused by disruption of the coronal magnetic field by a sudden increase in gas pressure.

(4) The CME is then driven out. Simultaneously the resultant changes in the lower coronal magnetic field may trigger a substantial fresh energy release, which results in the flare. However, there may be insufficient energy remaining in the energy reservoir, or the storage mechanism may now be too stable, for this to occur.

(5) If a major flare occurs, a flare-induced blast wave is set up, which produces a strong shock with associated type II radio emission.

A schematic representation of this sequence is given in Figure 9. If particle acceleration occurs with access to open field lines, it is unlikely that a CME will be initiated

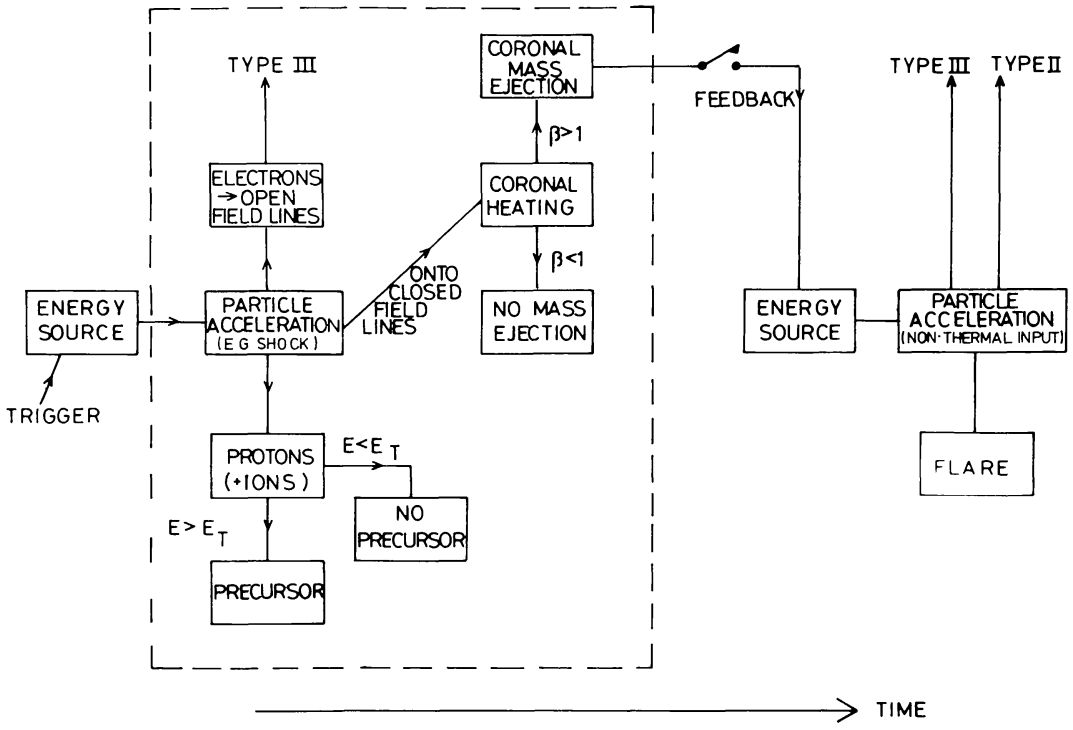

Fig. 9. A schematic representation of the model we propose to account for the precursor activity preceding coronal mass ejections, shown inside the dotted box. There may be feedback to the energy source which will cause a major flare to occur.

as the energy will escape. The lack of type III emission for five of the prime events in Table I suggests either that electrons were not accelerated significantly or that the field lines were closed in the low corona, or probably both. If the acceleration is via small shocks, then the bulk of the energy in non-thermal particles should reside in the protons,

which explains the absence of a hard X-ray burst at this time. This could account for the large number of type III bursts seen in the absence of X-ray emission.

With regard to the downward moving protons, if the spectrum extends above the threshold energy E_T for penetration to the chromosphere, some heating should occur, leading to soft X-ray emission from remote points corresponding to the footpoints of the coronal arch. However, if this threshold is not reached there will be no precursor activity, although there may still be a CME. The next branch point in Figure 9 is related to the magnitude of the energy loss within the closed field lines. Clearly unless the tension in the magnetic field lines can be reduced sufficiently nothing dramatic will happen; there will be evidence of coronal activity, but there will be no CME.

Finally, as the CME moves outwards, there may be acceleration at the shock formed at its leading edge. The general disturbance of the field lines will drive the reconnection process (Heyvaerts *et al.*, 1977) harder, causing more energy release. Because the reconnecting fields cannot be precisely the same fields involved in the earlier reconnection process which led to the precursor activity, then the flare is generally not seen at precisely the same place as one of the footpoints of the original structure. Also, because this structure has been opened up by the CME, a remote brightening will not normally be observed. Backward streaming particles from the outward propagating shock may feed back to the reconnection region and form a seed population of non-thermal particles for further acceleration. Type III bursts would be expected at this time as the field lines have opened up.

Acknowledgements

The Hard X-Ray Imaging Spectrometer was built as a collaboration between the Space Research Laboratory, Utrecht, and the Department of Space Research, Birmingham. We have benefitted from discussions with Drs. M. Dryer and R. Illing. Part of this work was completed while one of us (GMS), was enjoying the hospitality of the Institut für Astronomie, E.T.H. Zürich.

References

Basri, G. B., Linsky, J. L., Bartoe, J.-D. F., Brueckner, G., and van Hoosier, M. E.: 1979, *Astrophys. J.* **230**, 924.

Bell, R. A.: 1978, *Monthly Notices Roy. Astron. Soc.* **182**, 147.

Canfield, R. C. and Cook, J. W.: 1978, *Astrophys. J.* **225**, 650.

Dennis, B. R., Frost, K. J., Orwig, L. E., Kiplinger, A., Dennis, H. E., Gibson, B. R., Kennard, G. S., and Tolbert, A. K.: 1983, NASA T.M. 84998.

Dryer, M.: 1982, *Space Sci. Rev.* **33**, 233.

Elliot, H.: 1964, *Planetary Space Sci.* **12**, 657.

Gary, D. E., Dulk, G. A., House, L. L., Illing, R., Sawyer, C., Wagner, W. J., McLean, D. J., and Hildner, E.: 1984, *Astron. Astrophys.* **134**, 122.

Gergely, T.: 1984, in M. A. Shea, D. F. Smart, and S. M. P. McKenna-Lawlor (eds.), *Proc. STIP Symposium on Solar/Interplanetary Intervals*, Engineering International, Inc., Huntsville, AL., U.S.A., p. 237.

Harrison, R. A., Simnett, G. M., Hoyng, P., LaFleur, H., and Van Beek, H. F.: 1984, in M. A. Shea, D. F. Smart, and S. M. P. McKenna-Lawlor (eds.), *Proc. STIP Symposium on Solar/Interplanetary Intervals*, Engineering International, Inc., Huntsville, AL., U.S.A., p. 287.

Harrison, R. A., Waggett, P. W., Bentley, R. D., Phillips, K. J. H., Bruner, M., Dryer, M., and Simnett, G. M.: 1985, *Solar Phys.* **97**, 387.
Heyvaerts, J., Priest, E. R., and Rust, D. M.: 1977, *Astrophys. J.* **216**, 123.
House, L. L., Wagner, W. J., Hildner, E., Sawyer, C., and Schmidt, H. U.: 1981, *Astrophys. J. Letters* **244**, L117.
Jackson, B. V.: 1981, *Solar Phys.* **73**, 133.
Kerdraon, A., Pick, M., Trottet, G., Sawyer, C., Illing, R., Wagner, W. J., and House, L. L.: 1983, *Astrophys. J. Letters*, **265**, L19.
Lantos, P., Kerdraon, A., Rapley, C. G., and Bentley, R. D.: 1981, *Astron. Astrophys.* **101**, 33.
Lin, R. P. and Hudson, H. S.: 1976, *Solar Phys.* **50**, 153.
Machado, M. E., Avrett, E. H., Vernazza, J. E., and Noyes, R. W.: 1980, *Astrophys. J.* **242**, 336.
Najita, K. and Orrall, F. Q.: 1970, *Solar Phys.* **15**, 176.
Orrall, F. Q. and Zirker, J. B.: 1976, *Astrophys. J.* **208**, 618.
Pneuman, G. W.: 1980, *Solar Phys.* **65**, 369.
Rust, D. M., Simnett, G. M., and Smith, D. F.: 1985, *Astrophys. J.* **288**, 401.
Sawyer, C., Simnett, G. M., Erskine, F. T. III., and Gergely, T.: 1984, in M. A. Shea, D. F. Smart, and S. M. P. McKenna-Lawlor (eds.), *Proc. STIP Symposium on Solar/Interplanetary Intervals*, Engineering International, Inc., Huntsville, AL., U.S.A., p. 237.
Sawyer, C., Wagner, W. J., House, L. L., and Illing, R. M. E.: 1985, submitted to *J. Geophys. Res.*
Simnett, G. M.: 1985, *Astron. Astrophys.* **145**, 139.
Stewart, R. T.: 1976, *Solar Phys.* **50**, 437.
Stewart, R. T.: 1984, *Solar Phys.* **92**, 343.
Švestka, Z.: 1970, *Solar Phys.* **13**, 471.
Van Beek, H. F., Hoyng, P., LaFleur, H., and Simnett, G. M.: 1980, *Solar Phys.* **65**, 39.
Wagner, W. J.: 1983, *Adv. Space Res.* **2**, No. 11, 203.
Wagner, W. J. and MacQueen, R. M.: 1983, *Astron. Astrophys.* **120**, 136.
Webb, D. F., Krieger, A. J., and Rust, D. M.: 1976, *Solar Phys.* **48**, 159.